

The application and interpretation of Keeling plots in terrestrial carbon cycle research

D. E. Pataki,¹ J. R. Ehleringer,¹ L. B. Flanagan,² D. Yakir,³ D. R. Bowling,¹ C. J. Still,^{4,5} N. Buchmann,⁶ J. O. Kaplan,⁶ and J. A. Berry⁷

Received 16 December 2001; revised 17 April 2002; accepted 3 September 2002; published 7 March 2003.

[1] Photosynthesis and respiration impart distinct isotopic signatures to the atmosphere that are used to constrain global carbon source/sink estimates and partition ecosystem fluxes. Increasingly, the “Keeling plot” method is being used to determine the carbon isotope composition of ecosystem respiration ($\delta^{13}\text{C}_R$) in order to better understand the processes controlling ecosystem isotope discrimination. In this paper we synthesize emergent patterns in $\delta^{13}\text{C}_R$ by analyzing 146 Keeling plots constructed at 33 sites across North and South America. In order to interpret results from disparate studies, we discuss the assumptions underlying the Keeling plot method and recommend standardized methods for determining $\delta^{13}\text{C}_R$. These include the use of regression calculations that account for error in the x variable, and constraining estimates of $\delta^{13}\text{C}_R$ to nighttime periods. We then recalculate $\delta^{13}\text{C}_R$ uniformly for all sites. We found a high degree of temporal and spatial variability in C_3 ecosystems, with individual observations ranging from -19.0 to -32.6‰ . Mean C_3 ecosystem discrimination was 18.3‰ . Precipitation was a major driver of both temporal and spatial variability of $\delta^{13}\text{C}_R$, suggesting (1) a large influence of recently fixed carbon on ecosystem respiration and (2) a significant effect of previous climatic effects on $\delta^{13}\text{C}_R$. These results illustrate the importance of water availability as a key control on atmospheric $^{13}\text{CO}_2$ and highlight the potential of $\delta^{13}\text{C}_R$ as a useful tool for integrating environmental effects on dynamic canopy and ecosystem processes. **INDEX TERMS:** 0315 Atmospheric Composition and Structure: Biosphere/atmosphere interactions; 0322 Atmospheric Composition and Structure: Constituent sources and sinks; 1615 Global Change: Biogeochemical processes (4805); 1694 Global Change: Instruments and techniques; 3322 Meteorology and Atmospheric Dynamics: Land/atmosphere interactions; **KEYWORDS:** carbon cycle, carbon isotopes, ecosystem respiration, carbon dioxide, terrestrial ecosystems

Citation: Pataki, D. E., J. R. Ehleringer, L. B. Flanagan, D. Yakir, D. R. Bowling, C. J. Still, N. Buchmann, J. O. Kaplan, and J. A. Berry, The application and interpretation of Keeling plots in terrestrial carbon cycle research, *Global Biogeochem. Cycles*, 17(1), 1022, doi:10.1029/2001GB001850, 2003.

1. Introduction

[2] The existing and potential feedbacks between terrestrial ecosystem processes and atmospheric CO_2 concentrations remain one of the largest uncertainties in our understanding of the global carbon cycle. The balance of

photosynthesis and ecosystem respiration appears to be strongly influenced by interannual variability in climate with discernable effects on global CO_2 concentrations [Bousquet *et al.*, 2000], although the exact mechanisms remain unclear. In order to explain the current regional distribution of terrestrial carbon sources and sinks we must gain a better understanding of the factors controlling Net Ecosystem Exchange (NEE) of CO_2 both on short time-scales and over long periods.

[3] NEE is now measured around the world in numerous ecosystems as part of FLUXNET, the international network of eddy covariance sites [Baldocchi *et al.*, 2001]. Key products of FLUXNET studies include responses of NEE and its components to environmental variables. Methods to partition NEE into Gross Primary Production (GPP) and respiration are numerous, and include estimating ecosystem respiration from nighttime measurements [Goulden *et al.*, 1996], scaling cuvette measurements [Law *et al.*, 1999], and applying process models [Baldocchi and Meyers, 1998]. Because of the potentially different effects of photosyn-

¹Department of Biology, University of Utah, Salt Lake City, Utah, USA.

²Department of Biological Sciences, University of Lethbridge, Lethbridge, Alberta, Canada.

³Department of Environmental Science, Weizmann Institute of Science, Rehovot, Israel.

⁴Berkeley Atmospheric Sciences Center, University of California, Berkeley, Berkeley, California, USA.

⁵Now at Department of Geography, University of California, Santa Barbara, Santa Barbara, California, USA.

⁶Max Planck Institute for Biogeochemistry, Jena, Germany.

⁷Department of Plant Biology, Carnegie Institution of Washington, Stanford, California, USA.

thesis and respiration on the isotopic composition of CO₂, analysis of air samples for the carbon and oxygen isotope ratios of carbon dioxide within and above the canopy has also been proposed as a tool for understanding the components of NEE [Baldocchi *et al.*, 1996; Flanagan and Ehleringer, 1998; Yakir and Wang, 1996]. This isotopic approach has now been combined with eddy covariance measurements [Bowling *et al.*, 2001] and offers an additional and independent means of partitioning photosynthesis and ecosystem respiration interannually and across FLUXNET sites.

[4] A comprehensive effort to study the biophysical processes that control whole-canopy and whole-ecosystem discrimination at a number of sites around the world may contribute not only to ecosystem-scale carbon cycle studies, but also to global estimates of carbon sources and sinks. The carbon isotope ratios of CO₂ in the atmosphere are used to partition the regional carbon sources/sinks inferred from atmospheric CO₂ measurements and physical transport models [Battle *et al.*, 2000; Ciais *et al.*, 1995; Francey, 1985; Keeling *et al.*, 1989]. The mechanistic basis for this approach is the influence of photosynthetic enrichment and respiratory depletion of ¹³CO₂ on the isotopic composition of the atmosphere. Therefore, C₃ and C₄ photosynthetic discrimination as well as the isotopic disequilibrium between current photosynthetic fixation and respired CO₂ must be modeled for terrestrial ecosystems at large spatial scales [Fung *et al.*, 1997; Kaplan *et al.*, 2002; Lloyd and Farquhar, 1994]. Process models that predict the isotopic composition of ecosystems are based on the leaf-level discrimination equations given by Farquhar *et al.* [1989] and Farquhar and Sharkey [1982], and are just beginning to be tested with ecosystem-scale data [Buchmann and Kaplan, 2001]. As modeling efforts continue, a new understanding of the processes controlling isotopic discrimination at ecosystem and larger scales is likely to emerge. To facilitate this process, the Global Change and Terrestrial Ecosystems (GCTE) core project of the International Geosphere Biosphere Programme (IGBP) has initiated an international network to work in concert with the existing FLUXNET effort. The Biosphere-Atmosphere Stable Isotope Network (BASIN) consists of studies measuring the isotopic composition of ecosystems and their trace gas fluxes at FLUXNET sites as well as other sites around the world. Like FLUXNET, BASIN serves as an archive for network data and initiates international synthesis and modeling efforts on key ecosystem processes (<http://gctefocus1.org/basin.html>).

[5] A consideration of experimental protocols, sampling schemes, and common data interpretation is essential to any effort to integrate data across disparate studies. General reviews of the application of isotopic techniques to ecosystem gas exchange measurements have been published previously [Flanagan and Ehleringer, 1998; Yakir and Sternberg, 2000]. In this paper we focus on one of the primary methods of extracting information on the isotopic composition of ecosystem fluxes. The “Keeling plot” method, first employed by Keeling [1958, 1961], is now commonly used and often cited, but seldom explicitly analyzed. We discuss the assumptions underlying the Keel-

ing plot method in detail using data compiled from the literature and the BASIN online database in order to propose a common framework for the collection and interpretation of Keeling plot data. We then calculate Keeling plot intercepts in a uniform manner across all sites and present a synthesis of the patterns of the carbon isotope ratio of ecosystem respiration.

2. Keeling Plot Approach

[6] The basis of the Keeling plot method is conservation of mass. The atmospheric concentration of a gas in the canopy and adjacent boundary layer reflects the combination of some background atmospheric concentration and variable amounts of that gas added by sources in the ecosystem,

$$c_a = c_b + c_s, \quad (1)$$

where c_a , c_b , and c_s are, respectively, the atmospheric CO₂ concentration measured in the ecosystem, the background CO₂ concentration, and the additional concentration component produced by the source, which has raised atmospheric CO₂ concentration above background. In this paper, we focus on CO₂ as the atmospheric gas and respiration as the source, but the same arguments and application will apply to other gases such as water vapor [e.g., Moreira *et al.*, 1997], methane [e.g., Thom *et al.*, 1993], and other isotope ratios including ¹⁸O/¹⁶O and D/H (each application may have its own caveats).

[7] Given conservation of mass,

$$\delta^{13}C_a c_a = \delta^{13}C_b c_b + \delta^{13}C_s c_s, \quad (2)$$

where $\delta^{13}C$ represents the carbon isotope ratio of each CO₂ component. Combining equations (1) and (2),

$$\delta^{13}C_a = c_b (\delta^{13}C_b - \delta^{13}C_s) / (c_a - c_b) + \delta^{13}C_s, \quad (3)$$

where $\delta^{13}C_s$ is the integrated value of the CO₂ sources in the ecosystem. This is illustrated graphically in Figure 1.

[8] The linear regression approach was first used by Keeling [1958, 1961] to interpret fluctuations in the $\delta^{13}C$ values of ambient CO₂ and to identify the sources that contributed to increases in atmospheric CO₂ in a forest canopy. Later studies extended this approach to other forest ecosystems [Buchmann *et al.*, 1997a, 1997b; Flanagan *et al.*, 1996; Harwood *et al.*, 1999; Lancaster, 1990; Quay *et al.*, 1989; Sternberg *et al.*, 1989] and agricultural sites [Buchmann and Ehleringer, 1998]. Estimates of the carbon isotope composition of ecosystem respiration ($\delta^{13}C_R$) are essential for approaches using concentration and isotope measurements to partition net ecosystem fluxes of CO₂ into their photosynthetic and respiratory components [Bowling *et al.*, 2001; Yakir and Wang, 1996]. Similar partitioning approaches have been used to distinguish root versus microbial respiration [Lin *et al.*, 1999; Rochette and Flanagan, 1997; Rochette *et al.*, 1999] and transpiration versus evaporation [Harwood *et al.*, 1999; Moreira *et al.*, 1997].

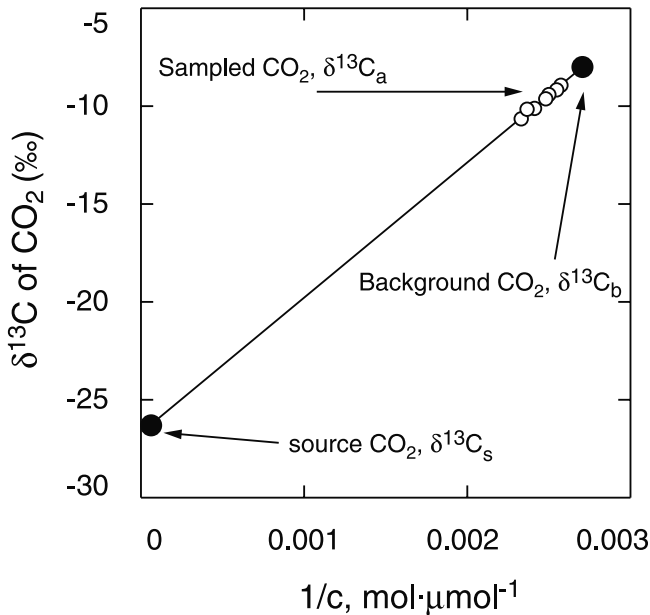


Figure 1. Graphical illustration of the Keeling plot method given as equation (3) in the text. The carbon isotope composition of two endpoints of source CO₂ ($\delta^{13}C_s$) and well-mixed, background atmospheric CO₂ ($\delta^{13}C_b$) are shown in solid circles. The carbon isotope composition of sampled air ($\delta^{13}C_a$) is shown by open circles. Isotope ratios are plotted against the inverse of CO₂ concentration (c). Note the distance of the samples from the intercept.

[9] More recently, *Buchmann et al.* [1998a] suggested that at equilibrium the isotopic composition of CO₂ respired from ecosystems and the carbon isotope discrimination by an ecosystem (Δ_e) were related as

$$\Delta_e = (\delta^{13}C_T - \delta^{13}C_R) / (1 + \delta^{13}C_R), \quad (4)$$

where $\delta^{13}C_T$ is the free troposphere value. In work by *Buchmann et al.* [1998a], daytime and nighttime data were combined to estimate $\delta^{13}C_R$ as they were not found to be different; in other words, there was no detectable disequilibrium between nighttime respiratory effects on atmospheric $\delta^{13}CO_2$ and daytime effects. It is often likely to be the case that ecosystem gas exchange is not at complete isotopic equilibrium. The dynamics of photosynthetic processes respond to climatic drivers on scales of hours to days, whereas ecosystem respiration is a mixture of various components responding to carbon inputs on scales of days to years. Yet to a first approximation for regional studies, assuming that photosynthetic and respiratory processes are at equilibrium may be reasonable for C₃- or C₄- only ecosystems.

[10] Regional scale biological discrimination has also been estimated with similar atmospheric approaches [*Bakwin et al.*, 1998; *Lloyd et al.*, 2001, 1996]. In these cases, carbon isotope discrimination was assessed by measuring simultaneous changes to the concentration and stable isotope composition of CO₂ within the convective boundary layer (CBL).

The CBL integrates the effects of photosynthesis, respiration, and turbulent transport of CO₂ over landscapes, thus increasing the spatial scale of discrimination measurements [*Lloyd et al.*, 1996; *Nakazawa and Sugawara*, 1997].

[11] It is important to recognize that the model described by equations (1)–(3) involves two basic assumptions. First, we assume that a simple mixing of only two gas components is considered (a source S and the bulk background B). Second, we assume that the isotope ratio of these two components does not change over the course of the observation. It is rare for these two assumptions to hold true in a strict sense under natural field conditions. Rather, researchers have found appropriate points in time and space for which these assumptions are acceptable. Below we outline recommendations for minimizing error in the use of the Keeling plot for assessing the carbon isotope composition of respiration.

3. Statistical Analysis

[12] An important consideration in constructing Keeling plots is which regression formulation to use. The standard (“Model I”) linear regression assumes that the independent variable (1/CO₂ concentration in this case) has no errors associated with it, or that these errors are under the experimenter’s control [*Sokal and Rohlf*, 1995]. Furthermore, Model I regression also assumes that errors in the dependent variable ($\delta^{13}C$ of atmospheric CO₂ in this case) are unrelated to the independent variable [*Laws*, 1997; *Sokal and Rohlf*, 1995]. These assumptions are violated when constructing a Keeling plot, as there are likely to be errors in estimating both $\delta^{13}C_R$ and CO₂ concentration that are related, as one is present in the other. In this case, if Model I regression is applied to determining the functional relationship between y and x , the slope is biased to smaller values, such that the intercept is biased to less negative values [*Friedli et al.*, 1987; *Sokal and Rohlf*, 1995; *Angleton and Bonham*, 1995; *Laws*, 1997].

[13] There are several alternative regression formulations that attempt to account for errors in both x and y variables (for discussions see *Sokal and Rohlf* [1995] and *Laws* [1997]). A simple and widely used technique in this class is the Model II or geometric mean regression (GMR, also known as the reduced or standard major axis regression [*Laws*, 1997; *Ricker*, 1973; *Sokal and Rohlf*, 1995]). The slope of a Model II regression is simply calculated as the slope of a Model I regression divided by the R-coefficient of the x and y variables. To illustrate the effect of regression method on the Keeling plot intercept, $\delta^{13}C_R$ was calculated (inappropriately) with Model I and (correctly) with Model II regression for 146 individual Keeling plots in the BASIN database (see Figure 2 for a map and list of all sites used in the analysis). Intercepts were sorted into plots where the r^2 of the Model II results was less than 0.95 and plots where r^2 was greater than 0.95. As r^2 approaches unity, the slope and therefore the intercept values from Model I and Model II converge, as shown in Figure 3. This is because Model II effectively splits the difference between the two Model I predictive slopes that can be calculated for any set of 1/CO₂ and $\delta^{13}C$ data: a regression of $\delta^{13}C$ on 1/CO₂ (i.e., y on x) or a regression of 1/CO₂ on $\delta^{13}C$ (x on y). *Laws* [1997] discusses this in further detail. However, as the correlation

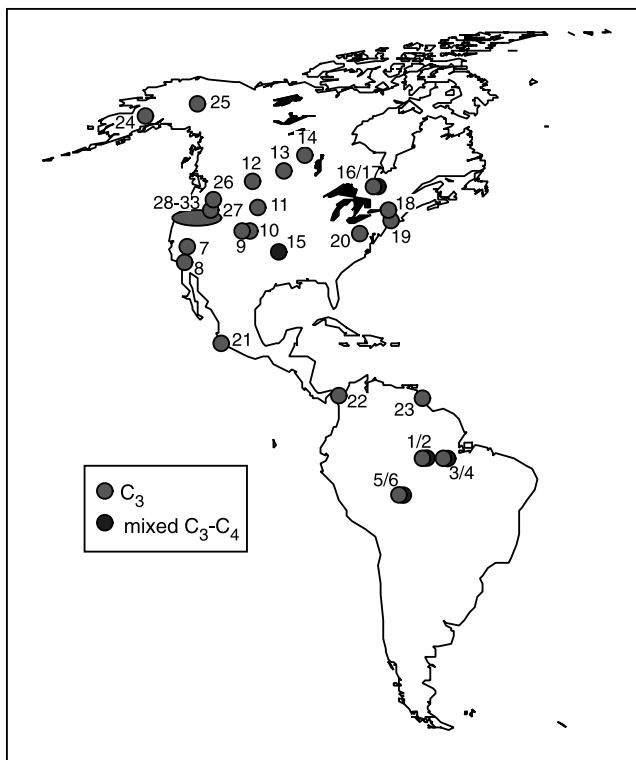
coefficient declines, the Model I intercept is systematically greater, or less negative, than the Model II intercept. In Figure 3, when r^2 was less than 0.95, the Model I intercept was up to 3‰ less negative than the Model II intercept, or 0.94‰ less negative on average (Figure 3).

[14] A potential problem with Model II is the assignment of error statistics. As *Laws* [1997] and *Angleton and Bonham* [1995] point out, calculating error bounds for the slope and intercept of a Model II regression is not the same as it is for a Model I regression. This appears to be a controversial topic within the statistics community. However, *Sokal and Rohlf* [1995] suggest using the standard error estimate from a Model I intercept to approximate the error estimate for a Model II intercept, which is followed here.

[15] Another formulation that incorporates errors in both CO_2 and $\delta^{13}\text{C}$ is the orthogonal distance regression (ODR), so named because the error function that is minimized calculates the distance between each data point and a line drawn orthogonal to the fitted line, rather than the distance between each data point and a line drawn orthogonal to the x axis as is done in standard linear regression [*Bakwin et al.*, 1995; *Laws*, 1997; *Press et al.*, 1992]. This method is more computationally intensive than the Model II method, but numerous computer programs based on the fitxy routine given by *Press et al.* [1992] are available on the internet. However, a substantial drawback of the ODR method is that it requires a priori estimates of the error in both $\delta^{13}\text{C}$ and CO_2 concentration, which are difficult to obtain.

4. Sampling Approaches

[16] Perhaps the simplest Keeling plot application and the first to have been applied [*Keeling*, 1958, 1961] was the use



of nighttime air samples to estimate the $\delta^{13}\text{C}$ value of respired CO_2 in an ecosystem. It is assumed in this case that when photosynthesis has ceased at night, only ^{13}C -depleted, respired CO_2 is added to the atmosphere, and that $\delta^{13}\text{C}$ of both background and respired CO_2 are constant during that time. Many of the potential sources of error in applying the Keeling approach can be considered under these conditions.

4.1. Multicomponent Systems

[17] Clearly, respired CO_2 originates from different sources including above and below ground respiration, and autotrophic and heterotrophic components. This may potentially violate the assumption of mixing only two compo-

Figure 2. (opposite) Location of sites used in this analysis. Data sources: 1 and 2: C_3 primary forest and mixed C_3 - C_4 pasture in Manaus, Brazil, details given by *Ometto et al.* [2002]; 3 and 4: C_3 primary forest and mixed C_3 - C_4 pasture in Santarem, Brazil, details given by *Ometto et al.* [2002]; 5 and 6: C_3 primary forest and mixed C_3 - C_4 pasture in Ji Parana, Brazil, details given by *Ometto et al.* [2002]; 7: coniferous forest in Yosemite National Park, California, details given by *Lancaster* [1990]; 8: mixed coniferous-deciduous forest in Cuyamaca Rancho State Park, California, details given by *Lancaster* [1990]; 9: deciduous forest in Red Butte canyon, Utah, details given by *Buchmann et al.* [1997b]; 10: deciduous and coniferous forests near Kamas, Utah, details given by *Buchmann et al.* [1997b]; 11: coniferous forest near Hamilton, Montana, details given by *Lancaster* [1990]; 12: C_3 grassland near Lethbridge, Alberta, from L.B. Flanagan (unpublished data, 1999); 13: coniferous and deciduous forests at the BOREAS Southern Study Area, details given by *Flanagan et al.* [1996, 1998]; 14: coniferous and deciduous forests at the BOREAS Northern Study Area, details given by *Flanagan et al.* [1996, 1998]; 15: mixed C_3 - C_4 grassland at the Konza Prairie Long-Term Ecological Research Site, Kansas, from L.B. Flanagan (unpublished data, 1998); 16 and 17: coniferous forest and corn crop near Ottawa, Ontario, from L.B. Flanagan (unpublished data, 1998); 18: deciduous forest near Barnard, Vermont, details given by *Lancaster* [1990]; 19: deciduous forest in Harvard Forest, Massachusetts, from J.R. Ehleringer (unpublished data, 1991); 20: deciduous forest in Scotia Range, Pennsylvania, details given by *Lancaster* [1990]; 21: tropical forest in Chamela, Mexico, details given by *Lancaster* [1990]; 22: tropical forest in Barro-Colorado Island, Panama, details given by *Lancaster* [1990]; 23: tropical forest in Paracou, French Guiana, details given by *Buchmann et al.* [1997a]; 24: tundra ecosystem near Bethel, Alaska, details given by *Lancaster* [1990]; 25: tundra ecosystem near Toolik Lake, Alaska, details given by *Lancaster* [1990]; 26: coniferous forests near Seattle, Washington, details given by *Buchmann et al.* [1998b]; 27: coniferous forests at the Wind River Canopy Crane site, Washington, details given by *Fessenden and Ehleringer* [2002]; 28–33: various coniferous forests along the Oregon Transect for Ecological Research (OTTER), details given by *Bowling et al.* [2002]. See color version of this figure at back of this issue.

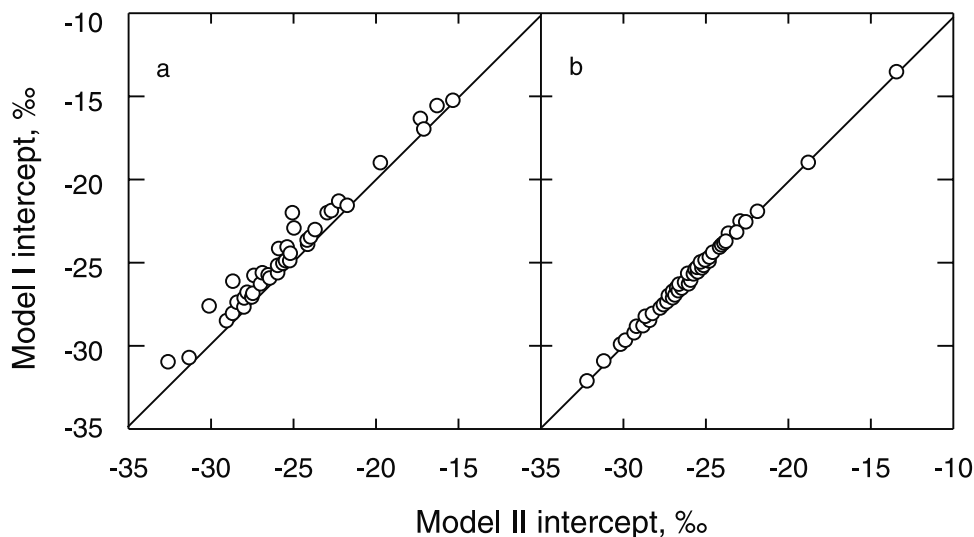


Figure 3. Comparison of Keeling plot intercepts from numerous study sites in North and South America as calculated with Model I (standard) regression and Model II (geometric mean) regression. (a) Data with Model II R-squares < 0.95 . (b) Data with Model II R-squares > 0.95 . The solid line is the 1:1 line.

nents in the linear model, but is not a concern if the $\delta^{13}\text{C}$ values of all these components are the same, or if their contributions to the total flux do not change proportionally over the time of sampling. In this case the spatial distribution of these fluxes dictates the locations of sample collection, depending on the question of interest. For instance, if we are interested in soil respiration and sample very near the ground (but not in the canopy), we will still have at least three CO_2 sources (background, heterotrophic respiration, and autotrophic respiration), but autotrophic and heterotrophic respiration with different $\delta^{13}\text{C}$ values may be represented by one well-mixed source of “soil” respired CO_2 above the ground. The estimated $\delta^{13}\text{C}_R$ in this case would be a flux-weighted mean value of the combined autotrophic and heterotrophic respiration belowground. If we have independent estimates of the specific $\delta^{13}\text{C}$ values of autotrophic and heterotrophic respiration, we could use equations (1)–(3) to partition soil respiration [e.g., *Yakir and Sternberg, 2000*]. Above and within the forest canopy, belowground and aboveground fluxes are combined in an estimate of whole ecosystem respiration; however, turbulent conditions often prevent a large buildup of CO_2 concentrations over rough canopies.

4.2. Footprint

[18] In the absence of herbaceous ground cover, measurements near the soil surface largely reflect the activity of a small patch of soil (small footprint) which may or may not be representative of the whole ecosystem. Although sampling footprint area increases with sampling height, maintaining the validity of the Keeling model assumptions may be difficult within the canopy. Under relatively stable conditions associated with canopy CO_2 buildup we may sample at different heights that reflect different mixtures of soil-respired, plant-respired and atmospheric CO_2 that may have distinct $\delta^{13}\text{C}$ values. If this is the case, the weighting of

each value on the final Keeling plot intercept may be affected by the chosen locations of sample collection. Such complications are usually ignored as differences in sampling various height profiles have not been well distinguished empirically. Additional research on sampling profiles is encouraged; currently, researchers should be aware of potential influence of sampling profile on the estimate of $\delta^{13}\text{C}_R$ and describe their sampling scheme accordingly.

[19] For regional-scale estimates representing very large footprints, aircraft measurements in well-mixed portions of the convective boundary layer (CBL) look to be promising. In a recent study in Siberia, *Lloyd et al. [2001]* found a correlation between $\delta^{13}\text{C}$ and $1/\text{CO}_2$ from aircraft flask measurements over very small CO_2 ranges of less than 3 ppm. As discussed below, when the Keeling plot is applied to small CO_2 ranges, the standard error around the intercept may be relatively large (1.6–5.6‰ in the *Lloyd et al. study*).

4.3. Temporal Variations in Isotopic Signals

[20] Recent studies question that the $\delta^{13}\text{C}$ in soil respired CO_2 is constant over timescales of days [*Ekblad and Högberg, 2001*]. Different organic substrates in the same plant have distinct $\delta^{13}\text{C}$ values, e.g., lipids are more depleted than carbohydrates by several per mil [*Benner et al., 1987*], and transition between different substrates for respiration may occur over short timescales (e.g., the diurnal cycle) [*Duranceau et al., 1999; Ghashghaie et al., 2001*]. Other recent studies also show that large changes in photosynthetic discrimination (on the order of 5‰) due to changes in environmental conditions are reflected in the $\delta^{13}\text{C}$ of respired CO_2 within a few days [*Bowling et al., 2002; Ekblad and Högberg, 2001*]. If the sampling period spans these temporal changes, the Keeling intercept will represent the intermediate of a family of lines with different slopes and intercepts. The best fit line may give a seemingly

“reasonable” value for the source, but one that may fall outside of the range of the actual value of the sources due to nonlinearities and other violations of the two-ended linear mixing model assumptions. To date, published Keeling plot data has generally been collected during time periods spanning 2–8 hours, although some have been collected over consecutive nights [Bowling *et al.*, 1999; Flanagan *et al.*, 1996]. We know of no reports of dynamic changes in the carbon isotope composition of ecosystem or soil respiration within these short periods, but additional studies are necessary to resolve the possibility of dynamic changes at this temporal scale.

[21] These recent findings of large changes in $\delta^{13}\text{C}_R$ over timescales of several days and longer provide examples of the potential complications in applying the Keeling-plot approach over long periods. However, they also demonstrate the importance of estimating nighttime $\delta^{13}\text{C}_R$ in ecosystems as a dynamic indicator of plant physiological response to change. Repeated Keeling plot sampling over time can provide valuable information on plant physiological function in response to environmental variables, as well as dynamic changes in heterotrophic substrates that influence the isotopic composition of soil respiration [Bowling *et al.*, 2002; Ekblad and Högberg, 2001].

4.4. Daytime Sampling

[22] Studies of the isotopic composition of ecosystem respiratory CO_2 should be limited to nighttime sampling. In the daytime, it is difficult to avoid the problems caused by multicomponent systems and isotopic signals that vary over time. Firstly, as the land surface heats in the morning and cools at night, the planetary boundary layer (PBL) becomes more dynamic, such that there may be rapid changes in the background signal during periods of rapid boundary layer depth change. Advection of air masses that have passed over other ecosystems (plant, marine, urban, industrial) will influence the Keeling mixing line if changes in $\delta^{13}\text{C}$ of background air occur during the measurement period. Respired CO_2 from the soil surface may also be re-fixed by the lower canopy, particularly in tropical forests [Lloyd *et al.*, 1996; Sternberg *et al.*, 1997, 1989]. For example, this occurs if photosynthesis begins before turbulent mixing disrupts the nighttime CO_2 profile, and it is likely to change over the time span of Keeling plot measurements.

[23] In addition, in many cases, photosynthesis and respiration may be at isotopic disequilibrium; that is, the change in the isotope ratio of atmospheric CO_2 caused by a unit of respiratory flux is not equivalent to the opposite change caused by a unit of photosynthetic fixation. This may be particularly true over short time periods such as one diurnal cycle; indeed, this is the basis for using isotopes to partition photosynthesis and respiration in ecosystem-scale flux studies [Bowling *et al.*, 2001; Yakir and Wang, 1996]. If photosynthetic and respiratory isotope effects on the atmosphere are not equal, combining nighttime and daytime measurements may create considerable uncertainty in the resulting intercept. To demonstrate the effect of diurnal sampling on the determination of δC_R , we have estimated δC_R in two ways for the data in the BASIN database, both

with daytime-only and nighttime-only data. Daytime and nighttime measurements were distinguished by calculating sunrise and sunset for each location by its latitudinal and longitudinal coordinates [Campbell and Norman, 1998], and sorting measurements based on their time of collection (there may be carryover effects of storage following the initiation or cessation of photosynthesis at dawn and dusk but these are difficult to determine). The results showed considerable scatter around the 1:1 line, such that the daytime estimate may differ from the nighttime-only value by as much as 5‰ in either direction (Figure 4). Hence, it appears that respiratory effects on atmospheric CO_2 commonly differ from recent photosynthetic effects, complicating the use of daytime data in Keeling plot estimates.

4.5. CO_2 Range

[24] The exclusion of daytime data or sampling over very short time periods (several hours) may present another difficulty: that of obtaining a sufficiently large CO_2 range for a Keeling plot analysis. A disadvantage of the Keeling plot approach is that it requires extrapolation far beyond the measured range of data to obtain the intercept (Figure 1), such that small uncertainties in the regression slope may lead to large uncertainties in the intercept [Tans, 1998]. In order to determine possible sampling strategies that reduce the standard error of the intercept, we analyzed the errors in the Keeling plot database using nighttime-only calculations with Model II regression (GMR).

[25] Assuming that measurement error has been minimized, two factors associated with sampling strategy are likely to influence the intercept. Intuitively, a broader CO_2 range in the air samples for a given Keeling plot should provide a better estimate of the intercept, as the distance from the data points to the y axis decreases with a larger x range. Secondly, simply increasing sample size (n) may provide a smaller error in $\delta^{13}\text{C}_R$.

[26] We plotted the standard error of the intercept as a function of the CO_2 range of the samples, sorting the data into categories corresponding to the number of air samples used in each plot (Figure 5). An inverse relationship was apparent. (Note that some data sets yielded very large standard errors exceeding 3‰.) A multiple, second-order, curvilinear regression showed that CO_2 range influenced the standard error of the intercept ($p < 0.0001$), but despite the autocorrelation between n and the standard error, the number of samples did not ($p = 0.57$). Thus, the error in the Keeling plot intercept is minimized by maximizing the range of CO_2 collected, regardless of how many samples are involved. The data in Figure 5 suggest that, in general, to reliably maintain a standard error in $\delta^{13}\text{C}_R$ below 1‰, a CO_2 range of approximately 75 ppm should be obtained, which occurs most commonly under stable conditions with relatively high respiratory fluxes.

4.6. Other Sampling Considerations

[27] Air samples for Keeling plot analysis have been collected in flasks ranging from 100 mL to 2 L in volume, such that the data set compiled for the present study represents a variety of air sample sizes. Previous work has shown that flask volume does not impact the quality of Keeling plot results [Ehleringer and Cook, 1998], so we

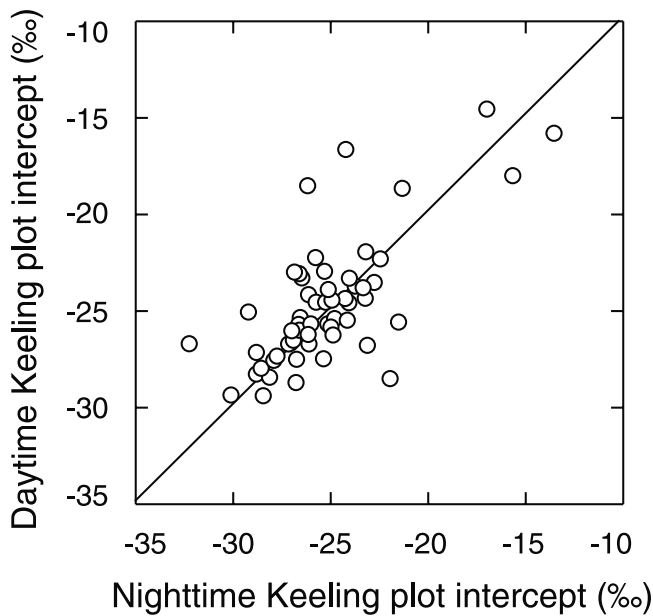


Figure 4. Comparison of Keeling plot intercepts derived from daytime-only and nighttime-only data. Data were sorted by calculating sunrise and sunset for each study site and applying the Model II, geometric mean regression calculation for each intercept. The solid line is the 1:1 line.

have treated the Keeling plot intercept as independent of flask volume in this analysis. It is also apparent that analytical methods and instrument precision are not constant across studies. For $\delta^{13}\text{C}$, precision values ranging from 0.03 to 0.13‰ have been reported, depending on whether dual inlet or continuous flow IRMS methods were used to measure ^{13}C in CO_2 [Buchmann *et al.*, 1997b; Ehleringer and Cook, 1998; Flanagan *et al.*, 1999]. As more than 95% of the Keeling plots analyzed in this study yielded standard errors exceeding 0.2‰ with a mean of 1.2‰, we consider the reported values for instrument precision to be of an acceptable magnitude.

5. Interpreting $\delta^{13}\text{C}_\text{R}$

[28] A major objective of a number of recent studies was to use estimates of $\delta^{13}\text{C}_\text{R}$ as a proxy for measurements of ecosystem-scale photosynthetic discrimination [Buchmann *et al.*, 1998b; Flanagan *et al.*, 1996; Flanagan and Ehleringer, 1998]. We have shown that applying the Keeling plot method during daytime conditions can be problematic on short, diurnal timescales (Figure 4). On longer timescales, this application is based on a number of assumptions of ecosystem processes and their associated isotopic fractionation. As discussed below, data from the BASIN network and information from several other recent studies can be used to address these assumptions and evaluate the consequences of using Keeling plot data to estimate ecosystem discrimination.

[29] First, it is critical to determine whether fractionation occurs during respiration. If this is not the case, the carbon isotope composition of respired CO_2 is dependent on the isotopic composition of the substrate molecules. While isotope secondary plant products are generally depleted in ^{13}C

compared to carbohydrates [Schmidt and Gleixner, 1998], on very long timescales, conservation of mass dictates that all fixed carbon will eventually return to the atmosphere. On shorter timescales relevant to ecosystem carbon exchange, i.e., days to years, we need to know the magnitude and consequence of secondary fractionation processes that might occur during plant and ecosystem respiration.

[30] Lin and Ehleringer [1997] observed that the $\delta^{13}\text{C}$ value of respired CO_2 released by incubated leaf protoplasts was not significantly different than that of the source carbohydrate (fructose, glucose, sucrose) supplied as a respiratory substrate. In such an experiment the source of the respiratory substrate is clear and unambiguous. For autotrophic respiration in a living leaf containing various substrates, it can be much more difficult to assess fractionation effects. Duranceau *et al.* [1999] and Ghashghaie *et al.* [2001] have shown that CO_2 respired in the dark was enriched in ^{13}C compared to leaf sucrose by 3–6‰. In work by Ghashghaie *et al.* [2001] the observed fractionation was variable with environmental conditions and differed between species. It is difficult to interpret the significance of these studies for an understanding of Keeling plot data, because it is unknown if the apparent fractionation results from isotope effects during decarboxylation reactions or isotopic differences among respiratory substrates. Similar difficulties apply to assessing fractionation in microbial respiration, which has

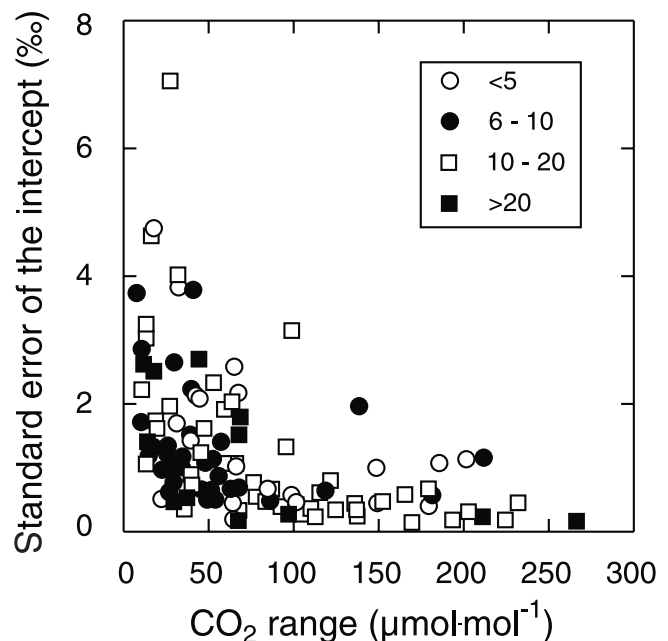


Figure 5. Standard error of the Keeling plot intercept as calculated from nighttime-only data with Model II, geometric mean regression is shown versus the range of CO_2 concentrations for each plot. Data are sorted into the number of data points in each regression as shown in the legend. A quadratic, multiple regression testing the effect of CO_2 range and number of data points on the standard error of the intercept showed that CO_2 range significantly influences the standard error ($p < 0.0001$), but there is no discernable effect of sample size ($p = 0.57$) or an interactive effect of CO_2 range and sample size ($p = 0.63$).

been proposed in several studies [Henn and Chapela, 2000; Schweizer et al., 1999]. Currently we suggest that at the ecosystem scale, there is insufficient evidence to conclude that fractionation during respiration has a large influence on the interpretation of Keeling plot data. However, this remains an active area of research.

[31] Second, the majority of recently respired carbohydrate was presumably fixed by sun leaves at the top of a plant canopy, and so its isotopic composition is not significantly affected by gradients in light intensity within the canopy, or source CO_2 that is depleted in ^{13}C [Berry et al., 1997; Buchmann et al., 2002]. The $\delta^{13}\text{C}$ of CO_2 respired by an entire ecosystem is more closely associated with that of sun foliage than with shade foliage across a variety of ecosystems (Figure 6). In addition, $\delta^{13}\text{C}_R$ of an entire ecosystem can be either more enriched or more depleted in ^{13}C than sun foliage. This is consistent with the idea that $\delta^{13}\text{C}_R$ may vary with short-term changes in environmental conditions, while leaf biomass $\delta^{13}\text{C}$ largely represents the value of photosynthetic discrimination at the time of leaf development. In other words, there is no reason to expect that the isotopic composition of ecosystem pools will be exactly equivalent to that of ecosystem fluxes.

[32] Ecosystems with a similar range of $\delta^{13}\text{C}$ values for soil organic matter also show a wide range of variation in ecosystem $\delta^{13}\text{C}_R$ (Figure 7). Soil organic matter is a carbon pool that represents an even longer temporal integration of primary production processes than that of individual leaves. In studies where the $\delta^{13}\text{C}$ of respired CO_2 was measured for both the entire ecosystem and the respiration flux from the soil, the soil flux was consistently enriched in ^{13}C compared to the entire ecosystem flux (Figure 7). Although enrichment of total soil organic matter (SOM) relative to litter inputs has been observed in many studies [Ehleringer et al., 2000], the carbon isotope composition of the pool of total SOM is a poor predictor of $\delta^{13}\text{C}$ of soil CO_2 flux [Buchmann et al., 1997a; Fessenden and Ehleringer, 2002], a large fraction of which originates from autotrophic respiration and heterotrophic respiration of a small, labile pool of carbon [Trumbore, 2000]. Root and stem tissues tend to be slightly ^{13}C enriched relative to leaf tissues, on the order of 1–3‰ in woody, C_3 plants [Boutton, 1996]. To the extent that $\delta^{13}\text{C}$ of soil CO_2 flux is influenced by the isotopic composition of root biomass, some enrichment in soil CO_2 efflux is expected relative to aboveground respiration.

6. Spatial and Temporal Patterns in $\delta^{13}\text{C}_R$

[33] Spatial variability in $\delta^{13}\text{C}_R$ has long been observed within C_3 ecosystems as a result of species-specific effects and environmental conditions. In this analysis, individual values for $\delta^{13}\text{C}_R$ in all studies containing only C_3 plants ranged from -19.0 to -32.6 ‰, with a mean of -26.2 ± 0.2 ‰ for 137 plots. The nighttime-only average over time obtained for each C_3 study ranged from -21.4 to -28.9 ‰, illustrating the large spatial variability in $\delta^{13}\text{C}_R$. Using the global average of -8 ‰ as a rough estimate of $\delta^{13}\text{C}_T$ in equation (4), the arithmetic mean Δ_e for the C_3 only data set was 18.3‰. This is somewhat lower than estimates of global C_3 discrimination of 20.0‰ by Quay et al. [1992]

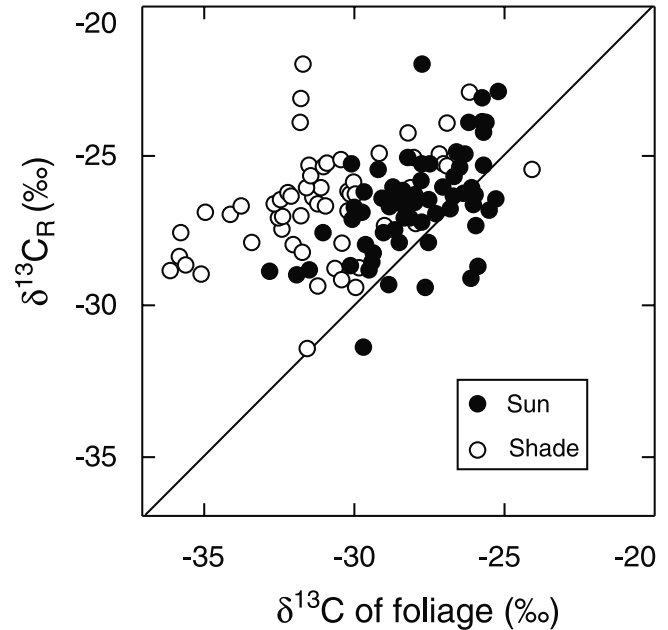


Figure 6. Carbon isotope composition ($\delta^{13}\text{C}$) of sun and shade foliage in relation to the carbon isotope composition of ecosystem respiration ($\delta^{13}\text{C}_R$) for a number of ecosystems throughout North and South America. Sun foliage values are the mean of measurements taken at the top of the canopy, and shade foliage is the mean of measurements taken in the bottom of the canopy and/or the understory. The solid line is the 1:1 line.

and Fung et al. [1997], but compares favorably with C_3 only estimates of 17.6–18.0‰ by Keeling et al. [1989], Tans et al. [1993], Lloyd and Farquhar [1994], and Buchmann and Kaplan [2001]. However, it is worth emphasizing that this is an ensemble average of data collected at various times, in some studies over multiple years. The range of Δ_e estimates from individual plots ranged from 11.2–25.5‰, with differences of up to 7‰ at a single study site from one year to the next. Thus, applying static estimates of biospheric discrimination to seasonal or interannual inversions of atmospheric CO_2 and $^{13}\text{CO}_2$ data may add to the uncertainty of temporal variability in source/sink estimates.

[34] Factors affecting the magnitude of $\delta^{13}\text{C}_R$ include the range of environmental parameters that control leaf c_i/c_a , such as light, temperature, and water availability, in addition to soil parameters that influence the isotopic composition of soil respiration, and the balance between above- and below-ground respiration. Models of photosynthetic discrimination have generated reasonable fits between predicted values and biomass or $\delta^{13}\text{C}_R$ data [Kaplan et al., 2002]. These models are based on leaf-level equations of environmental controls on photosynthesis and stomatal conductance [Lloyd and Farquhar, 1994] and the release of older, isotopically heavier carbon from soils and long-lived plant material [Buchmann et al., 1998a; Ciais et al., 1999; Fung et al., 1997]. However, considerable unexplained variability still exists, particularly as canopy-level estimates of photosynthetic discrimination are difficult to obtain in the field. It is useful to consider the key controls on $\delta^{13}\text{C}_R$ in a range of

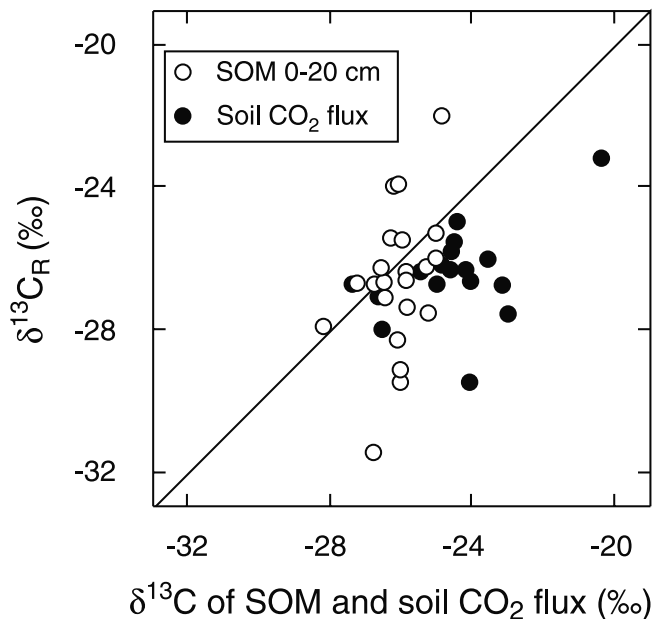


Figure 7. Carbon isotope composition ($\delta^{13}\text{C}$) of soil organic matter (SOM) at 0–20 cm and soil CO_2 flux in relation to the carbon isotope composition of ecosystem respiration ($\delta^{13}\text{C}_R$) for a number of ecosystems throughout North and South America. The isotopic composition of soil CO_2 flux was determined by sampling air from closed, flow-through soil respiration measurement systems with a number of different protocols. For further details see work by Flanagan *et al.* [1996], Buchmann *et al.* [1997a, 1998b], Flanagan *et al.* [1999], and Fessenden and Ehleringer [2002]. The solid line is the 1:1 line.

ecosystems both to improve modeling estimates and to further our understanding of ecosystem function.

[35] Trends among various biomes may highlight the importance of climate or plant functional type in influencing $\delta^{13}\text{C}_R$. We grouped the values for forest sites in the BASIN data set according to tropical, temperate broadleaf, temperate conifer, or boreal type to determine if latitude or biome was an important predictor of $\delta^{13}\text{C}_R$. No clear separations among biomes emerged (Figure 8). While differences in leaf $\delta^{13}\text{C}$ have been correlated with plant functional type within a given ecosystem [Brooks *et al.*, 1997], between broadleaf tropical forests and coniferous forests [Broadmeadow and Griffiths, 1993], and by latitude [Körner *et al.*, 1991], no simple and clear biome-dependent patterns emerged when all data were analyzed. Given the large range of studies and the additional variation introduced by the influence of soil respiration on $\delta^{13}\text{C}_R$, latitudinal and species effects may be obscured by other factors affecting spatial variability.

[36] Water availability is a major driver of plant productivity, and is also likely to be an important control of $\delta^{13}\text{C}_R$. Factors which cause short-term stomatal closure without a proportional reduction in photosynthesis should cause isotopic enrichment of organic material and subsequently $\delta^{13}\text{C}_R$. This has been demonstrated experimentally at the leaf-level as a positive relationship between water use efficiency (the ratio of carbon gain to water loss) and $\delta^{13}\text{C}$

of leaf material [Brugnoli *et al.*, 1998; Farquhar *et al.*, 1989; Farquhar and Richards, 1984]. We investigated the role of long-term water availability in influencing $\delta^{13}\text{C}_R$ by plotting mean $\delta^{13}\text{C}_R$ for each site versus mean annual precipitation (for sites which were only measured in a single year we plotted the annual precipitation for that year). This approach expands on the study by Bowling *et al.* [2002]. In the current study, a highly linear relationship was found for 17 study sites where average precipitation ranged from 230–2250 mm yr^{-1} , showing a large, long-term influence of water availability on the carbon isotope composition of respired CO_2 . However, in seven coniferous forest observations from the U.S. Pacific northwest region, where precipitation averaged 2400 mm yr^{-1} or greater, $\delta^{13}\text{C}_R$ was more enriched than predicted from the trend at other locations. Notably, of these forests the most enriched value was measured at the oldest forest, a 450-year-old stand at the Wind River Canopy Crane site in Washington, United States. Ryan and Yoder [1997] proposed that age-related factors other than drought stress cause stomatal closure in older forests (e.g., hydraulic limitation). The observations of enriched $\delta^{13}\text{C}_R$ in older coniferous forests are consistent with this observation [Bowling *et al.*, 2002; Fessenden and Ehleringer, 2002], although this has not been observed in all studies of these forests [Buchmann, 2000].

[37] Excluding the seven Pacific northwest conifer stand observations, precipitation explained 88% of the spatial

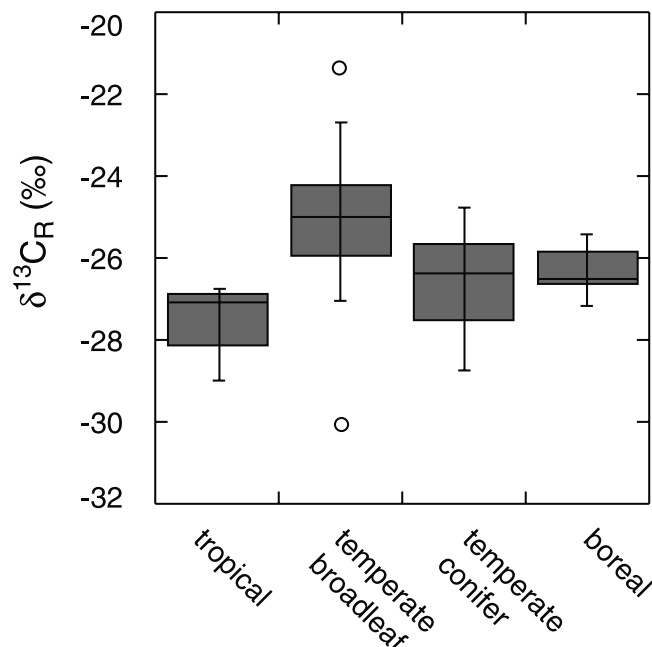


Figure 8. A box plot of data distribution of the carbon isotope composition of ecosystem respiration ($\delta^{13}\text{C}_R$) for four forest biome types in North and South America. The boxes enclose 50% of the data population, with the centerline showing the median value. The error bars show the upper/lower quartile + $(1.5 \times \text{interquartile distance})$. Points that lie outside of this range are shown by open circles. Sample sizes ranged from 6 to 17 for the boreal forests and temperate broadleaf forests, respectively.

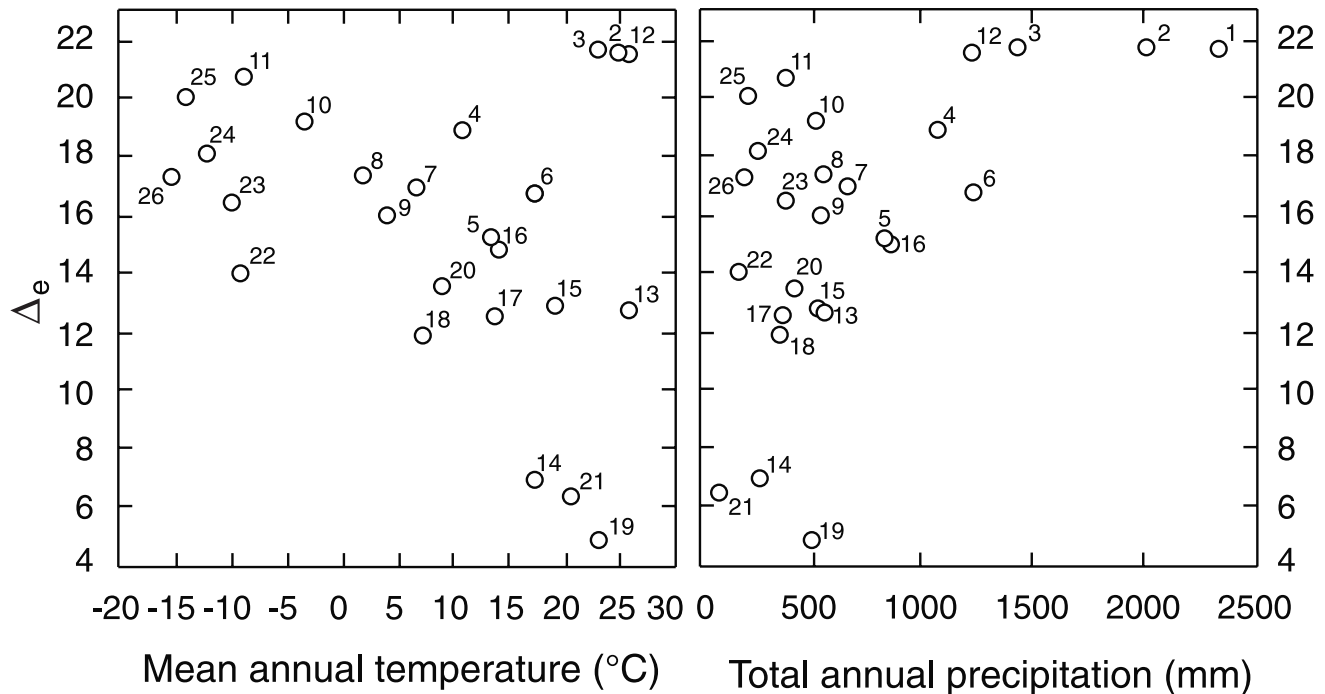


Figure 9. Ecosystem discrimination (Δ_e) versus mean annual temperature and precipitation as estimated by the BIOME 4 model for the world's biomes (note the four ecosystems which have a C_4 component in some areas): 1, tropical evergreen broadleaf forest; 2, tropical semi-evergreen forest; 3, tropical deciduous broadleaf forest and woodland; 4, temperate deciduous broadleaf forest; 5, temperate evergreen needleleaf forest; 6, warm-temperate evergreen broadleaf and mixed forest; 7, cool mixed forest; 8, cool evergreen needleleaf forest; 9, cool-temperate evergreen needleleaf and mixed forest; 10, cold evergreen forest; 11, cold deciduous forest; 12, tropical savanna (mixed C_3/C_4); 13, tropical xerophytic shrubland; 14, temperate xerophytic shrubland; 15, temperate sclerophyll woodland and shrubland; 16, temperate deciduous broadleaf savanna (mixed C_3/C_4); 17, temperate evergreen needleleaf open woodland; 18, cold parkland; 19, tropical grassland (mixed C_3/C_4); 20, temperate grassland (mixed C_3/C_4); 21, desert; 22, graminoid and forb tundra; 23, low- and high-shrub tundra; 24, erect dwarf-shrub tundra; 25, prostrate dwarf-shrub tundra; 26, cushion-forb, lichen, and moss tundra. From *Buchmann and Kaplan* [2001].

variability in $\delta^{13}C_R$, with a slope of $-2.0 \pm 0.2\text{‰ m}^{-1} \text{yr}^{-1}$ and an intercept of $-24.5 \pm 0.2\text{‰}$ ($p < 0.01$). *Bowling et al.* [2002] propose water stress-induced stomatal closure as the most likely explanation for this relationship across the forest types measured in that study. Further testing will be necessary to explicitly reject other potential mechanisms, such as moisture-related trends in the composition of soil respiration, or changes in the proportion of photosynthesis and respiration.

[38] To determine if current mechanistic models of isotope fractionation can reproduce the observed effect of precipitation across all ecosystems, the equilibrium global vegetation model BIOME4 was used to plot Δ_e (see equation (4)) against temperature and precipitation according to *Kaplan et al.* [2002]. The model predictions showed a correlation between Δ_e and both precipitation and temperature (Figure 9). Although there was more scatter and some curvilinearity in the precipitation relationship in contrast to the pattern shown in Figure 10, it should be noted that this exercise was global in scope and included a variety of biomes rather than forest ecosystems alone. Given this range, it appears that variations in Δ_e and $\delta^{13}C_R$ as a

function of water availability may be expected based on both measurements and modeling output.

[39] Recent studies have shown that a large fraction of respired CO_2 comes from the metabolism of recently fixed carbohydrates (fast cycling carbohydrate pools). *Ekblad and Högberg* [2001] observed a strong lagged correlation between atmospheric humidity and the $\delta^{13}C$ value of CO_2 released from the soil surface 2–4 days later in a boreal coniferous forest. *Bowling et al.* [2001] also have shown that the carbon isotope composition of CO_2 respired in coniferous forests in western Oregon was strongly correlated to the vapor pressure deficit (D) of air, consistent with expected responses of stomatal conductance and carbon isotope discrimination to humidity changes in these forests. The observed changes in $\delta^{13}C_R$ lagged behind shifts in D by 5–10 days, possibly because of the time necessary for recently fixed carbohydrate to be transported and metabolized in aboveground and belowground plant parts.

[40] Consistent with these observations, *Ometto et al.* [2002] have shown that seasonal changes in $\delta^{13}C_R$ values in a tropical evergreen forest were correlated with seasonal variation in precipitation inputs (Figure 11). The $\delta^{13}C_R$

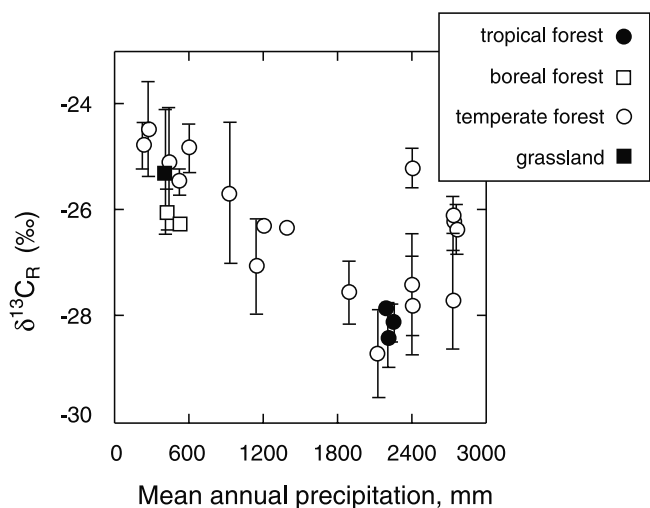


Figure 10. Mean carbon isotope composition of ecosystem respiration ($\delta^{13}\text{C}_R$) for study sites from various biomes in relation to the mean annual precipitation for that site. Bars indicate the standard error. For points without error bars, data were available for only 1 year and were plotted against the annual precipitation for that year.

values within Amazonian rain forests became more enriched in ^{13}C as monthly precipitation declined below 300 mm. Lower precipitation either reduced soil moisture and led to an increase in the stomatal limitation of photosynthesis during drought stress (lower c_i/c_a), or was associated with an increase in air temperature and D during the dry season, which would also contribute to an increase in the $\delta^{13}\text{C}$ of carbohydrates synthesized during photosynthesis. In addition, during a month of higher than normal precipitation (February 2000, 463 mm), $\delta^{13}\text{C}_R$ was enriched in ^{13}C (Figure 11). This was likely due to saturation of the soil and possible anaerobic stress effects on plants. Stomatal closure and reduced carbon isotope discrimination is a general stress response and has been demonstrated for plants exposed to flooding [Guy and Wample, 1984].

[41] The studies discussed above indicate that within an ecosystem, $\delta^{13}\text{C}_R$ appears to represent a multiple-day integration of carbon isotope discrimination during ecosystem photosynthesis, providing an excellent tool for analyzing canopy responses to fairly short-term changes in environmental conditions. These results have implications for inverse calculations of regional carbon sinks that use $^{13}\text{CO}_2$ to partition oceanic and terrestrial contributions. In these studies, estimates of disequilibrium effects are often based on the age of respired carbon in box models of ecosystem carbon pools [Ciais et al., 1995; Francey et al., 1995; Fung et al., 1997]. Two trends discussed here may change the interpretation of these results: (1) a larger than expected influence of recently fixed carbon and (2) a detectable impact of previous climatic events on $\delta^{13}\text{C}_R$.

[42] Intersite comparisons offer an opportunity to evaluate the controls over $\delta^{13}\text{C}_R$ on larger spatial and temporal scales. In this study, an analysis of the spatial distribution of $\delta^{13}\text{C}_R$ revealed an influence of long-term differences in climatic conditions (Figure 10). While these data were

insufficient to analyze the impacts of large-scale climatic event such as ENSO on discrimination, the finding that water availability has a large influence on mean $\delta^{13}\text{C}_R$ across a variety of ecosystems suggests that such patterns may indeed be observable at regional scales. Dynamic rather than static estimates of regional and global scale discrimination in inverse calculations may provide new information about seasonal and interannual variability in carbon sources and sinks.

7. Conclusions

[43] Spatially and temporally integrated values of ecosystem carbon isotope discrimination can be obtained from measurements of $\delta^{13}\text{C}$ of CO_2 respired by the entire ecosystem [Buchmann et al., 1998a; Flanagan and Ehleringer, 1998; Keeling, 1958]. There is accumulating evidence to suggest that a large fraction of respired CO_2 comes from the metabolism of recently fixed carbohydrates [Bowling et al., 2002; Ekblad and Högberg, 2001; Högberg et al., 2001; Malhi et al., 1999]. The $^{13}\text{C}/^{12}\text{C}$ ratio of this carbohydrate records information about plant physiological characteristics during the time that it was fixed, assuming no significant fractionation occurs during respiratory processes [Lin and Ehleringer, 1997]. Over longer periods, we expect that measurements of the carbon isotope composition of CO_2 respired from the entire ecosystem will represent an integrated measure of whole ecosystem discrimination [Bowling et al., 2002; Buchmann et al., 1998a; Flanagan et al., 1996; Flanagan and Ehleringer, 1998]. Analysis of trends across large regions can provide insight into biological controls over the isotopic composition of atmos-

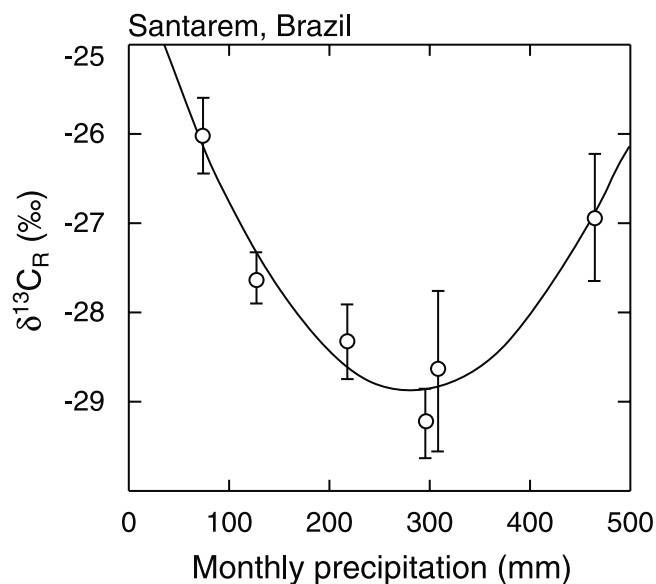


Figure 11. Carbon isotope composition of ecosystem respiration ($\delta^{13}\text{C}_R$) in relation to monthly precipitation in a tropical forest in Santarem, Brazil. Error bars represent the standard error. The curve represents a third-order polynomial fitted to the data: $Y = -23.789 - 3.719e-2 X + 7.1006e-5 X^2 - 1.1710e-8 X^3$, $r^2 = 0.954$. From Ometto et al. [2002].

phere. Further study is needed to elaborate the mechanisms influencing the magnitude of $\delta^{13}\text{C}_R$ and the disequilibrium between $\delta^{13}\text{C}_R$ and photosynthetic discrimination in a variety of ecosystems.

[44] To facilitate the integration of numerous data sets into a comprehensive understanding of terrestrial biosphere function, it is essential that methodology, analytical techniques, and interpretation be applied consistently. We have shown that standard, Model I regression introduces bias into the estimation of the Keeling plot intercept, such that techniques that account for error in the CO_2 parameter, such as Model II regression, must be applied. A large range (greater than 75 ppm) of CO_2 concentration during measurement period reduces the standard error in the intercept, and this standard error should always be reported. Although daytime data generally extends the measured CO_2 range, daytime measurements should only be included in Keeling plot analyses explicitly and with caution. Despite these caveats, we have shown that the isotopic composition of ecosystem carbon pools, such as leaf or soil organic material, is not equivalent to $\delta^{13}\text{C}_R$, so that Keeling plot estimates are the preferred method for assessing the carbon isotope composition of ecosystem fluxes. By applying common techniques to the estimation of the Keeling plot intercept, we can gain the maximum benefit from integrating estimates of $\delta^{13}\text{C}_R$ and Δ_e into a common framework for terrestrial carbon research.

[45] **Acknowledgments.** This manuscript developed from an informal discussion by members of the Biosphere-Atmosphere Stable Isotope Network (BASIN) at the American Geophysical Union meeting in San Francisco, California, in December 2000. We would like to thank the BASIN participants for all of their efforts. This work contributes to the Global Change and Terrestrial Ecosystems (GCTE) core project of the International Geosphere-Biosphere Programme (IGBP). Support for GCTE Focus 1 is provided by the NASA Earth Science Enterprise, with additional support for BASIN from NSF.

References

- Angleton, G. M., and C. D. Bonham, Least-squares regression vs. geometric mean regression for ecotoxicology studies, *Appl. Math. Comput.*, 72(1), 21–32, 1995.
- Bakwin, P. S., P. P. Tans, W. Ussler III, and E. Quesnell, Measurements of carbon dioxide on a very tall tower, *Tellus, Ser. B*, 47, 535–549, 1995.
- Bakwin, P. S., P. P. Tans, J. W. C. White, and R. J. Andres, Determination of the isotopic ($^{13}\text{C}/^{12}\text{C}$) discrimination by terrestrial biology from a global network of observations, *Global Biogeochem. Cycles*, 12(3), 555–562, 1998.
- Baldocchi, D., and T. Meyers, On using eco-physiological, micrometeorological and biogeochemical theory to evaluate carbon dioxide, water vapor and trace gas fluxes over vegetation: A perspective, *Agric. For. Meteorol.*, 90, 1–25, 1998.
- Baldocchi, D., R. Valentini, S. Running, W. Oechel, and R. Dahlman, Strategies for measuring and modelling carbon dioxide and water vapour fluxes over terrestrial ecosystems, *Global Change Biol.*, 2, 159–168, 1996.
- Baldocchi, D., E. Falge, and K. Wilson, A spectral analysis of biosphere-atmosphere trace gas flux densities and meteorological variables across hour to multi-year time scales, *Agric. For. Meteorol.*, 107, 1–27, 2001.
- Battle, M., M. L. Bender, P. P. Tans, J. W. C. White, J. T. Ellis, T. Conway, and R. J. Francey, Global carbon sinks and their variability inferred from atmospheric O_2 and $\delta^{13}\text{C}$, *Science*, 287, 2467–2470, 2000.
- Benner, R., M. L. Fogel, E. K. Sprague, and R. E. Hodson, Depletion of ^{13}C in lignin and its implications for stable carbon isotope studies, *Nature*, 329, 708–710, 1987.
- Berry, S. C., G. T. Vane, and L. B. Flanagan, Leaf $\delta^{13}\text{C}$ in *Pinus resinosa* trees and understory plants: Variation associated with light and CO_2 gradients, *Oecologia*, 109, 499–506, 1997.
- Bousquet, P., P. Peylin, P. Ciais, L. Quéré, P. Friedlingstein, and P. P. Tans, Regional changes in carbon dioxide fluxes of land and oceans since 1980, *Science*, 290, 1342–1346, 2000.
- Boutton, T. W., Stable carbon isotope ratios of soil organic matter and their use as indicators of vegetation and climate change, in *Mass Spectrometry of Soils*, edited by T. W. Boutton and S. Yamasaki, pp. 47–83, Marcel-Dekker, New York, 1996.
- Bowling, D. R., D. D. Baldocchi, and R. K. Monson, Dynamics of isotopic exchange of carbon dioxide in a Tennessee deciduous forest, *Global Biogeochem. Cycles*, 13(4), 903–922, 1999.
- Bowling, D. R., P. P. Tans, and R. K. Monson, Partitioning net ecosystem carbon exchange with isotopic fluxes of CO_2 , *Global Change Biol.*, 7, 127–145, 2001.
- Bowling, D. R., N. G. McDowell, B. J. Bond, B. E. Law, and J. R. Ehleringer, ^{13}C content of ecosystem respiration is linked to precipitation and vapor pressure deficit, *Oecologia*, 131, 113–124, 2002.
- Broadmeadow, M. S. J., and H. Griffiths, Carbon isotope discrimination and the coupling of CO_2 fluxes within forest canopies, in *Stable Isotopes and Plant Carbon-Water Relations*, edited by J. R. Ehleringer, A. E. Hall, and G. D. Farquhar, pp. 109–129, Academic, San Diego, Calif., 1993.
- Brooks, J. R., L. B. Flanagan, N. Buchmann, and J. R. Ehleringer, Carbon isotope composition of boreal plants: Functional grouping of life forms, *Oecologia*, 110, 301–311, 1997.
- Brugnoli, E., A. Scartazza, M. Lauteri, M. C. Monteverdi, and C. Maguas, Carbon isotope discrimination in structural and non-structural carbohydrates in relation to productivity and adaptation to unfavourable conditions, in *Stable Isotopes: Integration Of Biological, Ecological and Geochemical Processes*, edited by H. Griffiths, pp. 133–146, Bios, Oxford, England, 1998.
- Buchmann, N., Biotic and abiotic factors controlling soil respiration rates in *Picea abies* stands, *Soil Biol. Biochem.*, 32, 1625–1635, 2000.
- Buchmann, N., and J. R. Ehleringer, CO_2 concentration profiles, and carbon and oxygen isotopes in C_3 and C_4 crop canopies, *Agric. For. Meteorol.*, 89, 45–58, 1998.
- Buchmann, N., and J. O. Kaplan, Carbon isotope discrimination of terrestrial ecosystems—How well do observed and modeled results match?, in *Global Biogeochemical Cycles in the Climate System*, edited by E.-D. Schulze et al., pp. 253–268, Academic, San Diego, Calif., 2001.
- Buchmann, N., J.-M. Cuehl, T. S. Barigah, and J. R. Ehleringer, Interseasonal comparison of CO_2 concentrations, isotopic composition, and carbon dynamics in an Amazonian rainforest (French Guiana), *Oecologia*, 110, 120–131, 1997a.
- Buchmann, N., W.-Y. Kao, and J. Ehleringer, Influence of stand structure on carbon-13 of vegetation, soils, and canopy air within deciduous and evergreen forests in Utah, United States, *Oecologia*, 110, 109–119, 1997b.
- Buchmann, N., J. R. Brooks, L. B. Flanagan, and J. R. Ehleringer, Carbon isotope discrimination of terrestrial ecosystems, in *Stable Isotopes: Integration of Biological, Ecological and Geochemical Processes*, edited by H. Griffiths, pp. 203–221, Bios, Oxford, England, 1998a.
- Buchmann, N., T. M. Hinckley, and J. R. Ehleringer, Carbon isotope dynamics in *Abies amabilis* stands in the Cascades, *Can. J. For. Res.*, 28, 808–819, 1998b.
- Buchmann, N., J. R. Brooks, and J. R. Ehleringer, Predicting carbon isotope ratios of atmospheric CO_2 within forest canopies, *Funct. Ecol.*, 16, 49–57, 2002.
- Campbell, G. S., and J. M. Norman, *Environmental Biophysics*, Springer-Verlag, New York, 1998.
- Ciais, P., P. Tans, M. Trolier, J. White, and R. Francey, A large Northern Hemisphere terrestrial CO_2 sink indicated by the $^{13}\text{C}/^{12}\text{C}$ ratio of atmospheric CO_2 , *Science*, 269, 1098–1102, 1995.
- Ciais, P., P. Friedlingstein, D. S. Schimel, and P. P. Tans, A global calculation of the $\delta^{13}\text{C}$ of soil respired carbon: Implications for the biospheric uptake of anthropogenic CO_2 , *Global Biogeochem. Cycles*, 13(2), 519–530, 1999.
- Duranceau, M., J. Ghashghaie, F.-W. Badeck, E. Deleens, and G. Cornic, $\delta^{13}\text{C}$ of CO_2 respired in the dark in relation to $\delta^{13}\text{C}$ of leaf carbohydrates in *Phaseolus vulgaris* L. under progressive drought, *Plant Cell Environ.*, 22, 515–523, 1999.
- Ehleringer, J. R., and C. S. Cook, Carbon and oxygen isotope ratios of ecosystem respiration along an Oregon conifer transect: Preliminary observations based on small-flask sampling, *Tree Physiol.*, 18, 513–519, 1998.
- Ehleringer, J. R., N. Buchmann, and L. B. Flanagan, Carbon isotope ratios in belowground carbon cycle processes, *Ecol. Appl.*, 10(2), 412–422, 2000.
- Ekblad, A., and P. Höglberg, Natural abundance of ^{13}C in CO_2 respired from forest soils reveals speed of link between tree photosynthesis and root respiration, *Oecologia*, 127, 305–308, 2001.

- Farquhar, G. D., and R. A. Richards, Isotopic composition of plant carbon correlates with water-use efficiency of wheat genotypes, *Aust. J. Plant Physiol.*, *11*, 539–552, 1984.
- Farquhar, G. D., and T. D. Sharkey, Stomatal conductance and photosynthesis, *Annu. Rev. Plant Physiol.*, *33*, 317–345, 1982.
- Farquhar, G. D., J. R. Ehleringer, and K. T. Hubick, Carbon isotope discrimination and photosynthesis, *Annu. Rev. Plant Physiol. Plant Mol. Biol.*, *40*, 503–537, 1989.
- Fessenden, J. E., and J. R. Ehleringer, Age-dependent variations in $\delta^{13}\text{C}$ of ecosystem respiration across a coniferous forest chronosequence in the Pacific Northwest, *Tree Physiol.*, *22*, 159–167, 2002.
- Flanagan, L. B., and J. R. Ehleringer, Ecosystem-atmosphere CO_2 exchange: Interpreting signals of change using stable isotope ratios, *Trends Ecol. Evol.*, *13*(1), 10–14, 1998.
- Flanagan, L. B., J. Brooks, G. T. Varney, S. C. Berry, and J. R. Ehleringer, Carbon isotope discrimination during photosynthesis and the isotope ratio of respired CO_2 in boreal forest ecosystems, *Global Biogeochem. Cycles*, *10*(4), 629–640, 1996.
- Flanagan, L. B., J. R. Brooks, and J. R. Ehleringer, Photosynthesis and carbon isotope discrimination in boreal forest ecosystems: A comparison of functional characteristics in plants from three mature forest types, *J. Geophys. Res.*, *102*, 28,861–28,869, 1998.
- Flanagan, L. B., D. S. Kubien, and J. R. Ehleringer, Spatial and temporal variation in the carbon and oxygen stable isotope ratio of respired CO_2 in a boreal forest ecosystem, *Tellus, Ser. B*, *51*, 367–384, 1999.
- Francey, R. J., Cape Grim isotope measurements—A preliminary assessment, *J. Atmos. Chem.*, *3*, 247–260, 1985.
- Francey, R. J., P. P. Tans, C. E. Allison, I. G. Enting, J. W. C. White, and M. Troller, Changes in oceanic and terrestrial carbon uptake since 1982, *Nature*, *373*, 326–330, 1995.
- Friedli, H., U. Siegenthaler, D. Rauber, and H. Oeschger, Measurements of concentration, $^{13}\text{C}/^{12}\text{C}$ and $^{18}\text{O}/^{16}\text{O}$ ratios of tropospheric carbon dioxide over Switzerland, *Tellus, Ser. B*, *39*, 80–88, 1987.
- Fung, I., et al., Carbon 13 exchanges between the atmosphere and biosphere, *Global Biogeochem. Cycles*, *11*(4), 507–533, 1997.
- Ghashghaie, J., M. Duranceau, F.-W. Badeck, G. Cornic, M.-T. Adeline, and E. Deleens, $\delta^{13}\text{C}$ of CO_2 respired in the dark in relation to $\delta^{13}\text{C}$ of leaf metabolites: Comparison between *Nicotiana sylvestris* and *Helianthus annuus* under drought, *Plant Cell Environ.*, *24*, 505–515, 2001.
- Goulden, M. L., J. W. Munger, S. M. Fan, B. C. Daube, and S. C. Wofsy, Measurement of carbon storage by long-term eddy correlation: Methods and a critical assessment of accuracy, *Global Change Biol.*, *2*, 169–182, 1996.
- Guy, R. D., and R. L. Wample, Stable carbon isotope ratios of flooded and nonflooded sunflowers (*Helianthus annuus*), *Can. J. Bot.*, *62*(8), 1770–1774, 1984.
- Harwood, K. G., J. S. Gillon, A. Roberts, and H. Griffiths, Determinants of isotopic coupling of CO_2 and water vapour within a *Quercus petraea* forest canopy, *Oecologia*, *119*, 109–119, 1999.
- Henn, M. R., and I. H. Chapela, Differential C_3 - and C_4 -derived sucrose, *Appl. Environ. Microbiol.*, *66*(10), 4180–4186, 2000.
- Högberg, P., A. Nordgren, N. Buchmann, A. F. S. Taylor, A. Ekblad, M. Höglberg, G. Nyberg, M. Ottosson-Löfvenius, and D. J. Read, Large-scale forest girdling shows that current photosynthesis drives soil respiration, *Nature*, *411*, 789–792, 2001.
- Kaplan, J. O., I. C. Prentice, and N. Buchmann, The stable carbon isotope composition of the terrestrial biosphere: Modeling at scales from the leaf to the globe, *Global Biogeochem. Cycles*, *16*(4), 1060, doi:10.1029/2001GB001403, 2002.
- Keeling, C. D., The concentration and isotopic abundances of atmospheric carbon dioxide in rural areas, *Geochim Cosmochim. Acta*, *13*, 322–334, 1958.
- Keeling, C. D., The concentration and isotopic abundance of carbon dioxide in rural and marine air, *Geochim. Cosmochim. Acta*, *24*, 277–298, 1961.
- Keeling, C. D., R. B. Bacastow, A. F. Carter, S. C. Piper, T. P. Whorf, M. Heimann, W. G. Mook, and H. Roeloffzen, A three-dimensional model of atmospheric CO_2 transport based on observed winds, 1, Analysis of observational data, in *Aspects of Climate Variability in the Pacific and the Western Americas*, *Geophys. Monogr. Ser.*, vol. 55, edited by D. H. Peterson, pp. 165–236, AGU, Washington, D. C., 1989.
- Körner, C., G. D. Farquhar, and S. C. Wong, Carbon isotope discrimination by plants follows latitudinal and altitudinal trends, *Oecologia*, *88*, 30–40, 1991.
- Lancaster, J., Carbon-13 fractionation in carbon dioxide emitting diurnally from soils and vegetation at ten sites on the North American continent, Ph.D. thesis, Univ. of Calif. San Diego, San Diego, 1990.
- Law, B. E., D. D. Baldocchi, and P. M. Anthoni, Below-canopy and soil CO_2 fluxes in a ponderosa pine forest, *Agric. For. Meteorol.*, *94*, 171–188, 1999.
- Laws, E., *Mathematical Methods for Oceanographers*, John Wiley, New York, 1997.
- Lin, G., and J. R. Ehleringer, Carbon isotopic fractionation does not occur during dark respiration in C_3 and C_4 plants, *Plant Physiol.*, *114*, 391–394, 1997.
- Lin, G., J. R. Ehleringer, P. T. Rygielwicz, M. G. Johnson, and D. T. Tingey, Elevated CO_2 and temperature impacts on different components of soil CO_2 efflux in Douglas-fir terracosms, *Global Change Biol.*, *5*, 157–168, 1999.
- Lloyd, J., and G. D. Farquhar, ^{13}C discrimination during CO_2 assimilation by the terrestrial biosphere, *Oecologia*, *99*, 201–215, 1994.
- Lloyd, J., et al., Vegetation effects on the isotopic composition of atmospheric CO_2 at local and regional scales: Theoretical aspects and a comparison between a rain forest in Amazonia and a boreal forest in Siberia, *Aust. J. Plant Physiol.*, *23*, 371–399, 1996.
- Lloyd, J., et al., Vertical profiles, boundary layer budgets, and regional flux estimates for CO_2 and its $^{13}\text{C}/^{12}\text{C}$ ratio and for water vapor above a forest/bog mosaic in central Siberia, *Global Biogeochem. Cycles*, *15*(2), 267–284, 2001.
- Malhi, Y., D. D. Baldocchi, and P. G. Jarvis, The carbon balance of tropical, temperate and boreal forests, *Plant Cell Environ.*, *22*, 715–740, 1999.
- Moreira, M., L. Sternberg, L. Martinelli, L. Reynaldo, E. Barbosa, L. Bonates, and D. Nepstad, Contribution of transpiration to forest ambient vapour based on isotopic measurements, *Global Change Biol.*, *3*, 439–450, 1997.
- Nakazawa, T., and S. Sugawara, Aircraft measurements of the concentrations of CO_2 , CH_4 , N_2O , and CO and the carbon and oxygen isotopic ratios of CO_2 in the troposphere over Russia, *J. Geophys. Res.*, *102*(D3), 3843–3859, 1997.
- Ometto, P. H. B., L. B. Flanagan, L. A. Martinelli, M. Z. Moreira, N. Higuchi, and J. R. Ehleringer, Carbon isotope discrimination in forest and pasture ecosystems of the Amazon Basin, Brazil, *Global Biogeochem. Cycles*, *16*(4), 1109, doi:10.1029/2001GB001462, 2002.
- Press, W. H., S. A. Flannery, S. A. Teukolsky and W. T. Vetterling, *Numerical Recipes in C: The Art of Scientific Computing*, Cambridge Univ. Press, New York, 1992.
- Quay, P. D., S. L. King, D. Wilbur, S. Wofsy, and J. Richey, $^{13}\text{C}/^{12}\text{C}$ of atmospheric CO_2 in the Amazon Basin: Forest and river sources, *J. Geophys. Res.*, *94*(15), 18,327–18,336, 1989.
- Quay, P. D., B. Tilbrook, and C. S. Wong, Oceanic uptake of fossil fuel CO_2 : Carbon-13 evidence, *Science*, *256*, 74–79, 1992.
- Ricker, W. E., Linear regression in fishery research, *J. Fish. Res. Board Can.*, *30*, 409–434, 1973.
- Rochette, P., and L. B. Flanagan, Quantifying rhizosphere respiration in a corn crop under field condition, *Soil Sci. Soc. Am. J.*, *61*, 466–474, 1997.
- Rochette, P., L. B. Flanagan, and E. G. Gregorich, Separating soil respiration into plant and soil components using analyses of the natural abundance of carbon-13, *Soil Sci. Soc. Am. J.*, *63*, 1207–1213, 1999.
- Ryan, M. G., and B. J. Yoder, Hydraulic limits to tree height and tree growth, *Bioscience*, *47*(4), 235–242, 1997.
- Schmidt, H.-L., and G. Gleixner, Carbon isotope effects on key reactions in plant metabolism and ^{13}C -patterns in natural compounds, in *Stable Isotopes: Integration of Biological, Ecological and Geochemical Processes*, edited by H. Griffiths, pp. 13–25, Bios, Oxford, England, 1998.
- Schweizer, M., J. Fear, and G. Cadisch, Isotopic (^{13}C) fractionation during plant residue decomposition and its implications for soil organic matter studies, *Rapid Commun. Mass Spectrom.*, *13*, 1284–1290, 1999.
- Sokal, R. R., and F. J. Rohlf, *Biometry*, W. H. Freeman, New York, 1995.
- Sternberg, L. L., S. S. Mulkey, and J. S. Wright, Ecological interpretation of leaf carbon isotope ratios: Influence of respired carbon dioxide, *Ecology*, *70*(5), 1317–1324, 1989.
- Sternberg, L. L., M. Z. Moreira, L. A. Martinelli, R. L. Victoria, E. M. Barbosa, L. C. M. Bonates, and D. C. Nepstad, Carbon dioxide recycling in two Amazonian tropical forests, *Agric. For. Meteorol.*, *88*, 259–268, 1997.
- Tans, P. P., Oxygen isotopic equilibrium between carbon dioxide and water in soils, *Tellus, Ser. B*, *50*, 163–178, 1989.
- Tans, P. P., J. A. Berry, and R. F. Keeling, Oceanic $^{13}\text{C}/^{12}\text{C}$ observations: A new window on Ocean CO_2 uptake, *Global Biogeochem. Cycles*, *7*(2), 353–368, 1993.
- Thom, M., R. Bosinger, M. Schmidt, and I. Levin, The regional budget of atmospheric methane of a highly populated area, *Chemosphere*, *26*(1–4), 143–160, 1993.
- Trumbore, S., Age of soil organic matter and soil respiration: Radiocarbon constraints on belowground C dynamics, *Ecol. Appl.*, *10*(2), 399–411, 2000.

Yakir, D., and L. L. Sternberg, The use of stable isotopes to study ecosystem gas exchange, *Oecologia*, 123, 297–311, 2000.

Yakir, D., and X. F. Wang, Fluxes of CO₂ and water between terrestrial vegetation and the atmosphere estimated from isotope measurements, *Nature*, 380, 515–517, 1996.

J. A. Berry, Department of Plant Biology, Carnegie Institution of Washington, 290 Panama Street, Stanford, CA 94305, USA. (joeberry@biosphere.stanford.edu)

D. R. Bowling, J. R. Ehleringer, and D. E. Pataki, Department of Biology, University of Utah, 257 S 1400 E, Salt Lake City, UT 84112,

USA. (bowling@biology.utah.edu; ehleringer@biology.utah.edu; pataki@biology.utah.edu)

N. Buchmann and J. O. Kaplan, Max Planck Institute for Biogeochemistry, P.O. Box 10 01 64, 07701 Jena, Germany. (buchmann@bgc-jena.mpg.de; jed.Kaplan@bgc-jena.mpg.de)

L. B. Flanagan, Department of Biological Sciences, University of Lethbridge, 4401 University Drive, Lethbridge, Alberta, T1K3M4, Canada. (larry.Flanagan@uleth.ca)

C. J. Still, Department of Geography, University of California, Santa Barbara, Santa Barbara, CA 93101, USA. (cstill@geog.ucsb.edu)

D. Yakir, Department of Environmental Science, Weizmann Institute of Science, Rehovot 76100, Israel. (ciyakir@wis.weizmann.ac.il)

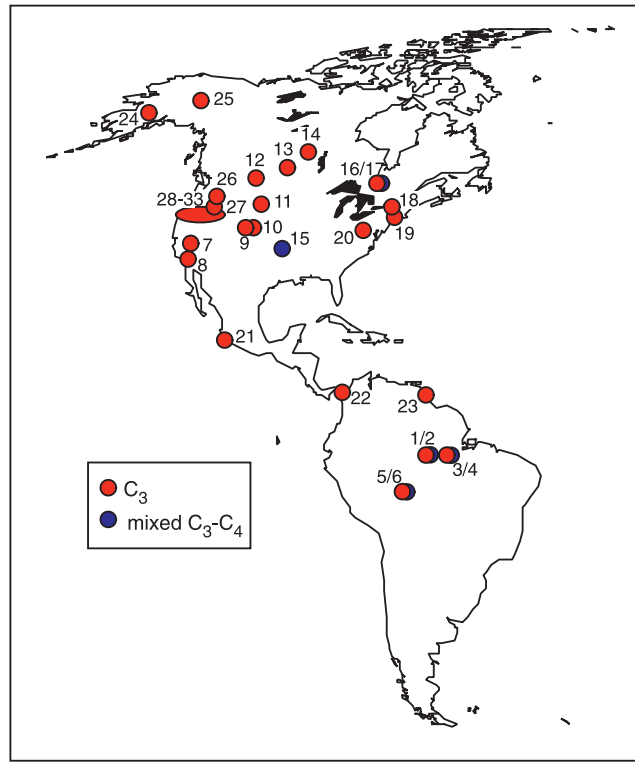


Figure 2. Location of sites used in this analysis. Data sources: 1 and 2: C_3 primary forest and mixed C_3 - C_4 pasture in Manaus, Brazil, details given by *Ometto et al.* [2002]; 3 and 4: C_3 primary forest and mixed C_3 - C_4 pasture in Santarem, Brazil, details given by *Ometto et al.* [2002]; 5 and 6: C_3 primary forest and mixed C_3 - C_4 pasture in Ji Parana, Brazil, details given by *Ometto et al.* [2002]; 7: coniferous forest in Yosemite National Park, California, details given by *Lancaster* [1990]; 8: mixed coniferous-deciduous forest in Cuyamaca Rancho State Park, California, details given by *Lancaster* [1990]; 9: deciduous forest in Red Butte canyon, Utah, details given by *Buchmann et al.* [1997b]; 10: deciduous and coniferous forests near Kamas, Utah, details given by *Buchmann et al.* [1997b]; 11: coniferous forest near Hamilton, Montana, details given by *Lancaster* [1990]; 12: C_3 grassland near Lethbridge, Alberta, from L.B. Flanagan (unpublished data, 1999); 13: coniferous and deciduous forests at the BOREAS Southern Study Area, details given by *Flanagan et al.* [1996, 1998]; 14: coniferous and deciduous forests at the BOREAS Northern Study Area, details given by *Flanagan et al.* [1996, 1998]; 15: mixed C_3 - C_4 grassland at the Konza Prairie Long-Term Ecological Research Site, Kansas, from L.B. Flanagan (unpublished data, 1998); 16 and 17: coniferous forest and corn crop near Ottawa, Ontario, from L.B. Flanagan (unpublished data, 1998); 18: deciduous forest near Barnard, Vermont, details given by *Lancaster* [1990]; 19: deciduous forest in Harvard Forest, Massachusetts, from J.R. Ehleringer (unpublished data, 1991); 20: deciduous forest in Scotia Range, Pennsylvania, details given by *Lancaster* [1990]; 21: tropical forest in Chamela, Mexico, details given by *Lancaster* [1990]; 22: tropical forest in Barro-Colorado Island, Panama, details given by *Lancaster* [1990]; 23: tropical forest in Paracou, French Guiana, details given by *Buchmann et al.* [1997a]; 24: tundra ecosystem near Bethel, Alaska, details given by *Lancaster* [1990]; 25: tundra ecosystem near Toolik Lake, Alaska, details given by *Lancaster* [1990]; 26: coniferous forests near Seattle, Washington, details given by *Buchmann et al.* [1998b]; 27: coniferous forests at the Wind River Canopy Crane site, Washington, details given by *Fessenden and Ehleringer* [2002]; 28–33: various coniferous forests along the Oregon Transect for Ecological Research (OTTER), details given by *Bowling et al.* [2002].